Introduction to Strongly correlated electron systems
&
Electrical and Structural Transitions in VO_2

國立高雄大學 www.nuk.edu.tw

Chin-Chung Yu

Strong correlated materials, correlated electron materials (CEMs)

Definition: 材料的電子的行為不能有效地運用非相互作用的原子系統來敘明。強關聯材料的電子結構的理論模型必須包括電子的相互關聯作用，才能作準確的物理預測。

大多數的特性源於材料的charge、spin、orbital的自由度(degree of freedom)、lattice之間的相互作用 。這些相互競爭的因素，通常會導致近簡併態(near degenerate states)的共存，並造成空間上的相不均勻(phase inhomogeneous)或在微米及奈米尺寸上造成多個domain structures。

⬇

造成研究上的困難度增加(巨觀的現象與微觀的理論模型無法吻合)

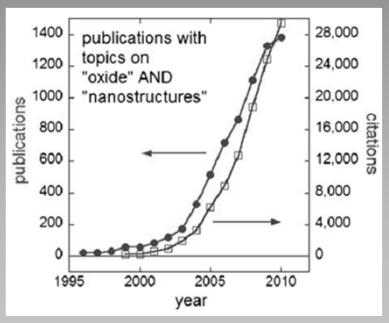

Growth of the number of publications with topics on "oxide" and "nanostructures" and their citations. Statistics from ISI Web of Knowledge

國立高雄大學 www.nuk.edu.tw

Chin-Chung Yu

Applications

特殊物理行為：
高溫超導high-TC superconductivity
超巨磁阻colossal magnetoresistance
非線性光學行為nonlinear optical behavior

Application of metal oxides:
透明電極、
高遷移率電晶體、
氣體傳感器、
光伏器件(photovoltaics; **光生伏打**，簡稱**光伏**，
字源photo: light，voltaics:
electricity)、
光子元件(photonic devices)、
能量收集和存儲元件、
非揮發性存儲器(non-volatile memories)

Phase inhomogeneity

Manganite is a mineral. Its composition is manganese oxide-hydroxide, MnO(OH), crystallizing in the monoclinic system (pseudo-orthorhombic).

Cuprate loosely refers to a material that can be viewed as containing copper anions. ex.: KCuO2, YBa2Cu3O7

在超巨磁阻的錳氧化物從鐵磁金屬相變至反鐵磁絕緣體，在這兩個相通常於從納米到微米尺寸下是共存的，其呈現一空間相的不均勻。

phase inhomogeneity 的理論解釋：intrinsic(內稟), extrinsic (外稟, external stimuli 外部刺激) mechanism
Intrinsic: elastically mediated phase coexistence (structure)
Extrinsic: lattice strain (epitaxial film, ex.: $La_{5/8-x}P_xCa_{3/8}MnO_3$ (x=0.3) (LPCMO)/ $NdGaO_3$ substrate)

Strain

Bulk single crystal: 如果相的不均勻在 strain-free, 單晶樣品中沒有出現，那麼這種樣品就是測試strain 對phase coexistence 的最佳平台。也就是說可以藉由external strain來調控phase inhomogeneity，如此就可以知道strain如何影響phase。

奈米結構：為一single domain、dislocation free。可以受coherent and continuously tunable external strain來調控。 可由臨場(in-situ)顯微實驗調變strain及溫度來觀察相轉變及domain動態行為。

bulk無機材料在塑性變形及斷裂前僅能維持非常低的非靜力應變（一般約<0.1 %）。在近期CEMs納米結構的合成(typically single crystals and dislocation free)提供了研究應變效應的新機會，因為這些奈米材料能夠維持一個額外的而且連續可調控之uniaxial strain。

Lattice strain/ strain tunning

- ➔ coupling between the charge, spin, and orbital degrees of freedom of electrons
- ➔ electrical, optical, and magnetic properties
- ➔ modify the properties of CEMs

VO_2

(1) origin of phase inhomogeneity in VO_2
(2) domain organization and manipulation
(3) Driving mechanism of the phase transition
(4) superelasticity in VO_2
(5) New phase stabilization under stress
(6) thermoelectric effects of the domain walls

Electrical and Structural Transitions in VO2

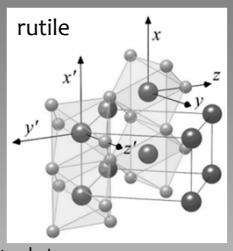

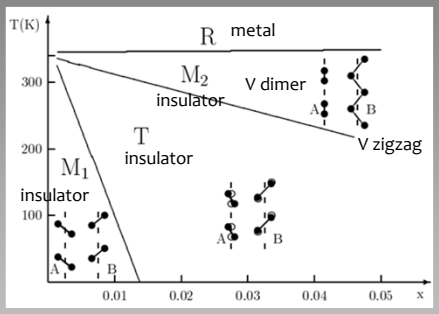

Phase diagram of V1−xCrxO2 according to Pouget an dLaunois. The distortion patterns of the metallic chains are given in the in sets (open circles in the T phase refer to the posit ions of the M2 phase)

The rutile structure of metallic VO_2 is based on a simple tetragonal lattice with space group $P4_2/mnm$ (D_{4h}^{14}, No. 136) [71, 27]. The metal atoms are located at the Wyckoff positions (2a): $(0,0,0)$, $(\frac{1}{2},\frac{1}{2},\frac{1}{2})$ and the oxygen atoms occupy the positions (4f): $\pm(u,u,0)$, $\pm(\frac{1}{2}+u,\frac{1}{2}-u,\frac{1}{2})$. The rutile structure is displayed in Fig. 4. According to McWhan *et al.* the lattice constants and the internal oxygen parameter are $a_R = 4.5546\,\text{Å}$, $c_R = 2.8514\,\text{Å}$ and $u = 0.3001$ [27]. These numbers will be used in the

國立高雄大學 www.nuk.edu.tw

Chin-Chung Yu

M1 Phases

In strain-free state,VO2 undergoes a first-order metal–insulator phase transition (MIT) and structural phase transition at T_C^o= 341 K.

high-temperature, tetragonal, metallic phase (rutile structure, R)

Temperature,
uniaxial strain,
doping(Cr, Al)

low-temperature, monoclinic, insulating phase (M1). the vanadium ions dimerized and these pairs tilt with respect to the R-phase c-axis (c_R).

Atom	Wyckoff positions	parameters		
		x	y	z
V	(4e)	0.242	0.975	0.025
O_1	(4e)	0.10	0.21	0.20
O_2	(4e)	0.39	0.69	0.29

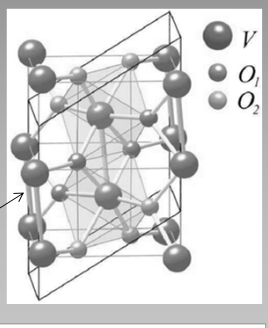

from M1 to R shrinks the specimen along c_R direction by ε_o~ 1%,
along the tetragonal a_R and b_R axe, the lattice expands by 0.6 and 0.1%, respectively,
causing a volume shrinkage of 0.3%

u

M2, T phases

Insulating monoclinic structure M2 phase can also be induced by doping with Cr or uniaxial compression perpendicular to c_R. In M2, only half of the vanadium atoms dimerize. while the other half form zigzag chains; therefore, it can be viewed as an intermediate structure between M1 and R.

from M1 to M2 expands it along c_R direction by ε_o~ 0.3%

Atom	Wyckoff positions	parameters		
		x	y	z
V_1	(4g)	0.0	0.7189	0.0
V_2	(4i)	0.2314	0.0	0.5312
O_1	(8j)	0.1482	0.2475	0.2942
O_2	(4i)	0.3969	0.0	0.2089
O_3	(4i)	0.1000	0.0	0.7987

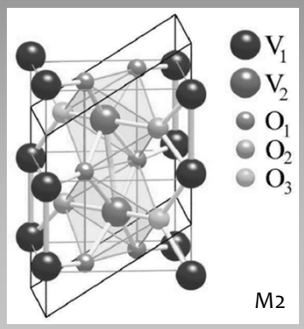

A triclinic phase (T) might also derive from the M1 structure, but only with a continuous change in lattice constant and angles.

Chin-Chung Yu

VO2 samples

The synthesis was performed using a vapor transport method: bulk VO2 powders were placed in a quartz boat in the center of a horizontal tube furnace.
The VO2 nanowire is 60 (±30) nm with lengths reaching up to >10um.

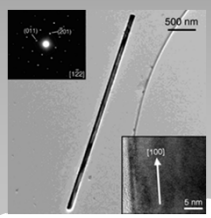

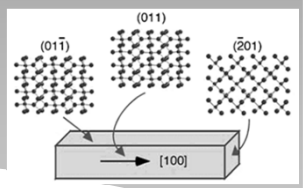

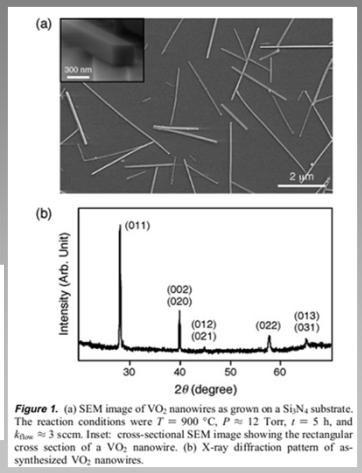

Figure 1. (a) SEM image of VO_2 nanowires as grown on a Si_3N_4 substrate. The reaction conditions were T = 900 °C, $P \approx 12$ Torr, t = 5 h, and $k_{flow} \approx 3$ sccm. Inset: cross-sectional SEM image showing the rectangular cross section of a VO_2 nanowire. (b) X-ray diffraction pattern of as-synthesized VO_2 nanowires.

monoclinic form of VO2 (JCPDS file 72-0514)

Chin-Chung Yu

Bulk, thin film, single-crystal nanometer size beam

Bulk crystals tend to crack across the MIT and degrade upon repeated cycling.

polycrystalline thin films often display a broadened transition associated with phase Inhomogeneity.

Single-crystal VO_2 nanometer and micrometer size beams will avoid the crackling of the specimens and eliminate the phase separation and domain formation that are widely observed in bulk and thin films, thus providing opportunities to investigate the intrinsic properties of VO_2 at the single domain level.

Chin-Chung Yu

single-crystal nanometer size beam with/ without strain

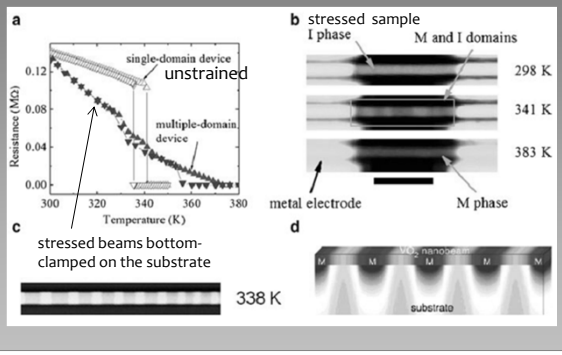

Conclusion:

That the multiple phase coexistence can be observed in stressed VO_2 beam but not in free-standing specimens suggest that the lattice strain be responsible to the phase inhomogeneity observed in polycrystalline VO_2 films.

The broadening of phase transition in VO_2 thin films is therefore a direct consequence of the phase inhomogeneity across the transition, which arises from the inevitable nonuniform local stress of the films.

(a) Four-probe resistance of single-crystal VO_2 beams as a function of temperature. The free-standing VO_2 beam shows single domain behavior, whereas the clamped beam shows multiple domains during the transition . (b) Optical images of the multiple-domain devices showing the coexistence of metallic (dark) and insulating (bright) domains at intermediate temperatures. The scale bar is 5 mm. (c) Optical image of clamped VO_2 at 338 K showing periodic metallic and insulating domains. The width of the VO_2 beam is around 1.5 mm. (d) Schematic diagram showing the periodic domain pattern of a VO_2 beam coherently strained on an SiO_2 substrate . Blue and red correspond to tensile and compressive strain, respectively. "M" denotes metallic phase.

Chin-Chung Yu

Formation of multiple domains

The multiple domain coexistence can be understood through analysis of energy minimization. Competition between strain energy in the elastically mismatched VO_2/substrate system and domain wall energy in the VO_2 resulted in multiple domains.

For a strained ferroelectric systems:
The total energy in unit nanobeam–substrate interface area is given by

$$E(\lambda) = \frac{\lambda\varepsilon}{\pi^3}\sum_{j=0}^{\infty}\frac{1-e^{-2(2j+1)\pi t/\lambda}}{(2j+1)^3} + \frac{\gamma t}{\lambda} + \frac{(f_M+f_I)t}{2}.$$

Here λ is the spatial period of the domain pattern, ε is the volume density of the elastic misfit energy, γ is the domain-wall energy per unit domain-wall area, t is the nanobeam thickness, and f_M and f_I are the free energy densities of the metallic and insulating phases, respectively.

卓越・活力・熱情 與
國立高雄大學
www.nuk.edu.tw

minimization of E(λ) ➔ λ.

Chin-Chung Yu

Domain dynamics & manipulation

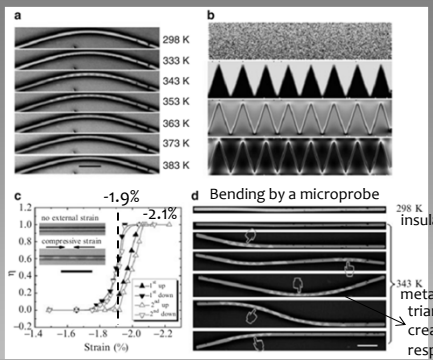

(a) Optical images of an array of triangular metallic domains nucleated and costabilized by tensile and compressive strain along a bent microbeam. (b) Phase-field modeling of domain formation in a bent VO_2 beam. From top to bottom: first, initial state of random phase distribution; second, equilibrium phase distribution at the natural MIT transition T_c^o ; third, equilibrium strain (ε_{xx}) distribution at T_c^o : yellow and dark green denote the maximum tensile and maximum compressive strain, respectively; forth, equilibrium strain energy density distribution: yellow denotes the highest strain energy density, dark green denotes the lowest. (c) Uniaxial compression reversibly induces a metal–insulator transition at room temperature. Here η is the fraction of metal phase along the beam. (d) Strain engineering domains in a flexible VO_2 microbeam. Scale bars in (a), (c), and (d) 10 um.

Process:
(1) insulating phase at room temperature
(2) increasing temperatures
(3) triangular metallic domains nucleate at the inner edge
(4) temperature was further increased
(5) metallic phase expanded toward the outer edge
(6) completely eliminated the insulating phase

inner edge ➔ compressive strain
the outer edge ➔ tensile strain

metallic triangular insulating domains was created in the high curvature region in response to the local tensile strain.

www.nuk.edu.tw

Chin-Chung Yu

Two-dimensional phase-field modeling

The total energy F(ϕ) is equal to the sum of bulk thermodynamic energy, interfacial (domain wall) energy, and strain energy:

$$F(\phi) = \int \left[f(\phi) + \frac{\beta^2}{2} |\nabla \phi|^2 + \frac{1}{2} C_{ijkl} \left(\varepsilon_{ij} - \varepsilon_{ij}^{T} \right) \left(\varepsilon_{kl} - \varepsilon_{kl}^{T} \right) \right] \, dA.$$

- ϕ denotes the phase
- f(f) describes the relative thermodynamic energy of the two phases (it is temperature dependent.)
- second term reflects the interfacial energy
- last term is the elastic energy where C is the elastic modulus tensor, ε is the strain, and ε^T is the lattice mismatch between the two phases.

(1) The periodic, triangular domain pattern, nearly completely relieves the strain energy in the bent beam, with some remnant strain at the triangular tips.
(2) competing effects of strain energy relaxation and interfacial energy ➔ smaller period results in more effective strain energy relief, but at the cost of introducing more interfacial area.

Chin-Chung Yu

Mechanism of metal-insulator transition (MIT)

Mott transition picture: (electron–electron correlation)
The insulating phase is a Mott insulator where the bandgap opens because of Coulomb blockade between strongly localized d electrons at the vanadium sites.

Peierls transition: (electron–lattice interaction, phonon-driven mechanism)
The bandgap exists because of lattice potential modulation by the vanadium dimerization.

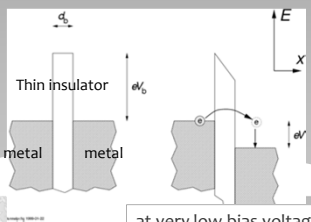

The tunnel junction capacitor is charged with one elementary charge by the tunnelling electron, causing a voltage buildup U=e/C. If the capacitance is very small, the voltage buildup can be large enough to prevent another electron from tunnelling. The electrical current is then suppressed at low bias voltages and the resistance of the device is no longer constant. The increase of the differential resistance around zero bias is called the Coulomb blockade.

at very low bias voltage & C is very small

Chin-Chung Yu

route A: constant stress (isobaric process,類似於液 - 汽相轉變時的等壓過程)
route B: constant temperature (isothermal process).
route C: combination of routes A and B

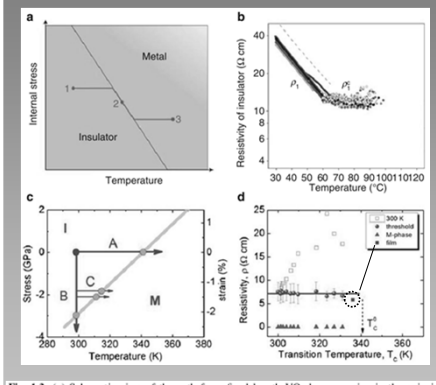

Fig. 1.3 (**a**) Schematic view of the path for a fixed length VO_2 beam moving in the uniaxial stress–temperature phase diagram [43]. (**b**) Resistivity of the insulating phase of VO_2 as a function of temperature. A constant resistivity (at 60–100°C) is observed when the system moves along the phase boundary [21]. (**c**) Isobaric (A), isothermal (B), and combined sequential processes (C) in the uniaxial stress–temperature phase diagram of VO_2 showing phase transition from the insulating (I) phase to metallic (M) phase. *Green dots* show schematically the position where the transition threshold is defined. (**d**) Measured resistivity of VO_2 beams at 300 K, at the threshold, and in M-phase, respectively. The error is mostly from uncertainties in determining the effective height and length of the microbeam. Also shown is the apparent threshold resistivity from a VO_2 thin film. The *horizontal line* shows the constancy of ρth in I phase

A constant resistivity of the insulating phase was observed when the system moves along the phase boundary.
The threshold resistivity (ρth) of the insulating phase right before the system switches to metallic phase and stays constant over a wide range.

In a Mott picture, the transition occurs when the density-dependent screening reaches a critical strength. As suggested by Mott theory, the density is the maximum semiconducting carriers coming from the insulating side, which is proportional to the threshold resistivity ρth. The observation that a constant critical free carrier
density has to be reached to trigger the insulator to metal transition indicates that the transition is fundamentally driven by electron–electron interactions.

Chin-Chung Yu

Superelasticity (超彈性, pseudoelasticity)

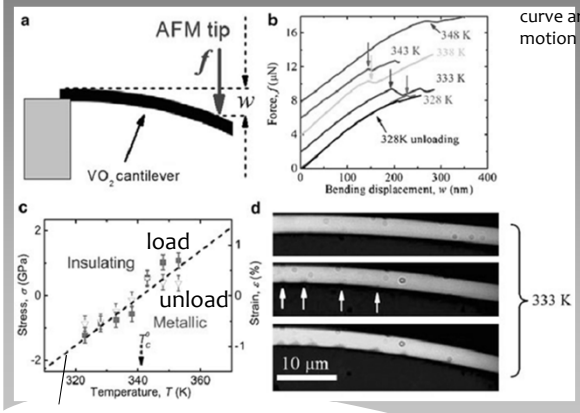

the nonlinearity and kinks in the f–w curve are related to the creation and motion of new domains.

In shape memory alloys, where an applied stress can cause a reversible phase transformation between the austenitic and martensitic phases of a crystal. The superelasticity originates from the reversible creation and motion of domain boundaries during the phase transformation.

Clapeyron equation

Chin-Chung Yu

New Phase Stabilization with Strain

Fabrication:
During the vapor-transport synthesis, single-crystal VO_2 beams grow on molten SiO_2 surface and could be clamped in different strain states varying from beam to beam, depending on local conditions during the cooling process.

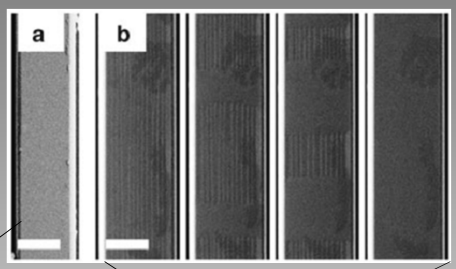

298, 323, 333, and 368 K (*left to right*)

The free-standing beams always have smooth, featureless surface that does not change as temperature increases Laue pattern of mXRD shows M1 structure at T<TC and R structure at T>TC.

The bottom-clamped beams, however, often show periodic stripes well aligned in parallel to the c_R direction at a period of ~150 nm.

Chin-Chung Yu

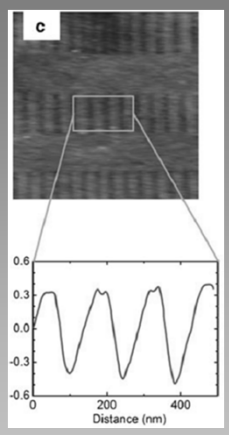

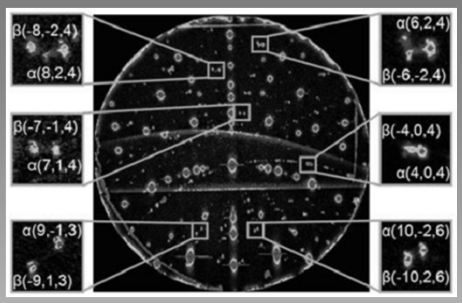

The room-temperature μXRD pattern of a bottom-clamed VO_2 beam indexed as a twinned monoclinic M2 phase (M2α/M2β).

$$M1 \rightarrow M1 + R \rightarrow M2 + R \rightarrow R$$

$$M2 \rightarrow M2 + R \rightarrow R$$

Chin-Chung Yu

Thermoelectric across the Metal–Insulator domain walls

$$R_{\mathrm{I}}(T) = R_{\mathrm{I}}^{0}\exp(E_{\mathrm{a}}/k_{\mathrm{B}}T)$$

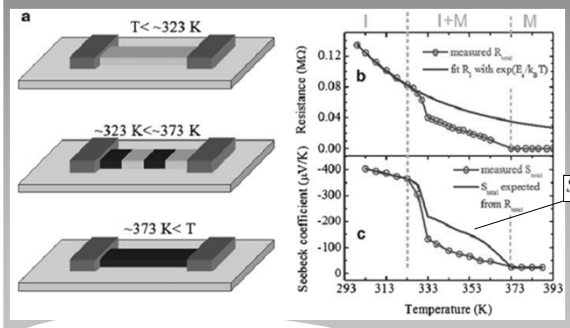

The thermoelectric effect can be measured from the same specimen with or without the Schottky junction, so that an accurate extraction of the net junction effect becomes possible.

$$S_{\mathrm{total}}(T) = x(T)S_{\mathrm{I}}(T) + [1 - x(T)]S_{\mathrm{M}}$$

$S_I(T)$ is extrapolated from the pure insulating phase regime and $S_M(T)$ is constant over the temperature range.

卓越・活力・熱情
國立高雄大學
www.nuk.edu.tw
Chin-Chung Yu